applied sciences

MDPI

Article

Numerical Simulation of Organic Pollution Migration in the Heterogeneous Aquifer and the Application of Chemotactic Bacteria for Remediation: A Case Study of a Chemical Contamination Site in Zhejiang Province, China

Shaohua Cao [1], Hailong Zhao [2,3], Xiaopu Wang [2,3], Xin Zhu [1] and Tao Long [1,*]

[1] State Environmental Protection Key Laboratory of Soil Environmental Management and Pollution Control, Nanjing Institute of Environmental Sciences, Ministry of Ecology and Environment, Nanjing 210042, China; zhuxin@nies.org (X.Z.)
[2] National Key Laboratory of Deep Oil and Gas, China University of Petroleum (East China), Qingdao 266580, China
[3] School of Petroleum Engineering, China University of Petroleum (East China), Qingdao 266580, China
* Correspondence: longtao@nies.org

Abstract: Groundwater pollution poses a significant threat to ecosystems and public safety. Traditional remediation methods have limitations, necessitating innovative approaches. This study integrates numerical modeling and bioremediation to address groundwater contamination in an industrial site. It explores the potential of chemotactic bacteria to enhance remediation efficiency. The research establishes groundwater pollutant transport models, analyzes flow fields, and assesses the distribution of various pollutants. The results demonstrate the effectiveness of chemotactic bacteria, particularly chemotactic bacteria that can rapidly adapt as the pollutant concentration decreases, the concentration of chemotactic bacteria in the low-permeability area has increased by 112%. This study provides insights into the practical application of bioremediation and the promising role of bacterial chemotaxis in treating contaminated groundwater.

Keywords: chemotactic bacteria; bioremediation; groundwater pollutant; numerical simulation

check for updates

Citation: Cao, S.; Zhao, H.; Wang, X.; Zhu, X.; Long, T. Numerical Simulation of Organic Pollution Migration in the Heterogeneous Aquifer and the Application of Chemotactic Bacteria for Remediation: A Case Study of a Chemical Contamination Site in Zhejiang Province, China. *Appl. Sci.* **2024**, *14*, 9924. https://doi.org/10.3390/app14219924

Academic Editor: José Miguel Molina Martínez

Received: 16 July 2024
Revised: 19 August 2024
Accepted: 30 August 2024
Published: 30 October 2024

Copyright: © 2024 by the authors. Licensee MDPI, Basel, Switzerland. This article is an open access article distributed under the terms and conditions of the Creative Commons Attribution (CC BY) license (https://creativecommons.org/licenses/by/4.0/).

1. Introduction

Groundwater is an irreplaceable and precious water resource that plays a vital role in environmental elements and ecosystems. Groundwater pollution has a severe impact on the ecological environment, hinders the progress of agriculture and industry, and poses a significant threat to the safety of the general population [1].

Traditional remediation methods primarily rely on the physical and chemical properties of non-aqueous pollutants, employing methods such as excavation, thermal desorption, vapor extraction, soil solidification, leaching, and redox reactions to treat pollutants in situ or ex situ. However, these methods often have a limited remediation scope, particularly yielding unsatisfactory results in deep, low-permeability zones, consuming significant energy, and risking soil structure disruption and secondary pollution [2–4]. More concerning is that these physical and chemical remediation methods, developed three decades ago, continue to be widely used. Therefore, the search for and establishment of more efficient, thorough, and environmentally friendly remediation methods is urgently needed.

Bioremediation utilizes biological resources such as microorganisms to degrade pollutants into harmless substances, offering advantages such as energy conservation and environmental friendliness. By degrading organic compounds, it provides sustainable energy for its own growth and proliferation, thus achieving effective remediation results [5–8]. In situ bioremediation, in particular, involves directly injecting microbial and enzyme preparations into the aquifer to degrade pollutants, proving to be economically

viable and widely applied in groundwater remediation projects internationally [9]. However, overcoming aquifer heterogeneity, with variations in porosity and permeability across different geological layers [10], remains a critical challenge in improving the efficiency of in situ bioremediation.

Chemotaxis is a capability evolved by many bacteria in the natural world, enabling them to sense concentration gradients of specific compounds (beneficial or harmful) and swim towards regions conducive to their survival and proliferation [11]. Several strains of naturally occurring harmless bacteria have been found not only to degrade petroleum pollutants but also to exhibit positive chemotactic responses to pollutants [12]. Studies at the population level have also been conducted. Pedit et al. [13] employed capillaries filled with micrometer-sized glass beads as a porous medium and observed the enrichment of the bacterium *Pseudomonas putida* (*P. putida*) G7 within the capillaries when naphthalene was present in the aqueous phase, a phenomenon not observed in the control group without naphthalene, thus providing early proof of the role of chemotactic bacteria in homogeneous porous media. Zhao et al. [14] used chemotaxis to assess the chemotactic behavior of the complete degrading bacterium *Pseudomonas* sp. ZWL73 and its conjugative transposon ZP8 toward 4-chloronitrobenzene (4CNB) and 12 compounds potentially related to 4CNB degradation, most of which could serve as substrates for ZWL73 growth. Qiao et al. [15] studied the chemotactic characteristics of the actinobacterium *Arthrobacter* sp. CN2, using nitrophenol as a substrate, and found a positive correlation between the bacterium's chemotaxis and nitrophenol concentration. Strobel et al. [16] created sandbox simulations to mimic cross-sectional homogeneous soil, making the experimental system closer to the actual environment, and observed the chemotactic migration of *P. putida* F1 toward the contaminated layer. Although these population-level studies have provided ample experimental and theoretical foundations for the application of chemotactic bacteria in porous media, their experimental systems remain overly simplistic, and they share a common limitation of being unable to replicate heterogeneous soil environments.

Due to the high cost of groundwater pollution site remediation and the potential for improper remediation methods to cause secondary pollution at the site, many scholars have used numerical simulation methods in recent years to predict the transport behavior of pollutants at the site. Xie et al. focused on the migration of manganese in groundwater using Visual MODFLOW and MT3DMS software in Xiangtan, China [17]. Alexander et al. employed the simulation models MODFLOW and MT3DMS, along with an optimization algorithm, to design an effective groundwater pollution management system for a decanting contaminated site [18]. Pongritsakda et al. suggested possibilities for predicting and remediating pollution at illegal waste dumping sites through numerical studies [19]. Shakeri et al. analyzed groundwater flow and nitrate contamination in the Karaj alluvial aquifer in Iran using MODFLOW and MT3DMS [20]. El-Aassar et al. integrated groundwater vulnerability assessment with contaminants transport modeling in the unsaturated zone in El-Sharqia, Egypt. Their study focused on aquifer vulnerability to pollution and the attenuation of contaminants transport through the vadose zone before groundwater seepage [21]. These studies have fully demonstrated the effectiveness of numerical simulation in formulating remediation strategies for groundwater pollution.

Therefore, this paper, in the context of on-site pollutant measurements, utilizes COMSOL 5.6 to establish a pollutant diffusion model and constructs a chemotactic bacteria migration model based on previous theories. This article assumes that the process of chemotactic bacteria decomposing pollutants is not considered; only the bacterial chemotactic accumulation is taken into account. The optimization goal is for chemotactic bacteria to enter the low-permeability areas more effectively. By optimizing the parameters in the chemotactic bacteria migration model, it aims to determine which aspects of the chemotactic bacteria's abilities should be enhanced to ensure a more outstanding performance in the face of heterogeneous soil environments. It explores optimization directions for bacterial chemotaxis in real-field remediation work.

2. Site Overview

2.1. Pollution Characteristics

The western side of the site was home to an enterprise established in 1993, primarily engaged in the production of pharmaceutical intermediates, with a main product being DL-hydroxybenzene. Production ceased in September 2010. On the eastern side, another enterprise began production in 2000, specializing in pharmaceutical raw materials, pharmaceutical intermediates, petrochemicals, and anti-mold agents for coatings, with major products including 2,4-dichlorofluorobenzene and 1,2-benzisothiazolin-3-one. Production at this facility also ceased in September 2010. According to preliminary investigations, the key pollutants of concern in the site's soil include 1,2,4-trichlorobenzene, 1,2-dichloroethane, 1,3-dichlorobenzene, 1,4-dichlorobenzene, 2,4-dinitrophenol, hexachlorobenzene, phenol, 2,4-dinitrochlorobenzene, 2,4-dinitrotoluene, and others. The groundwater contamination includes pollutants consistent with those found in the soil. The distribution of contaminants at the site is shown in Figure 1.

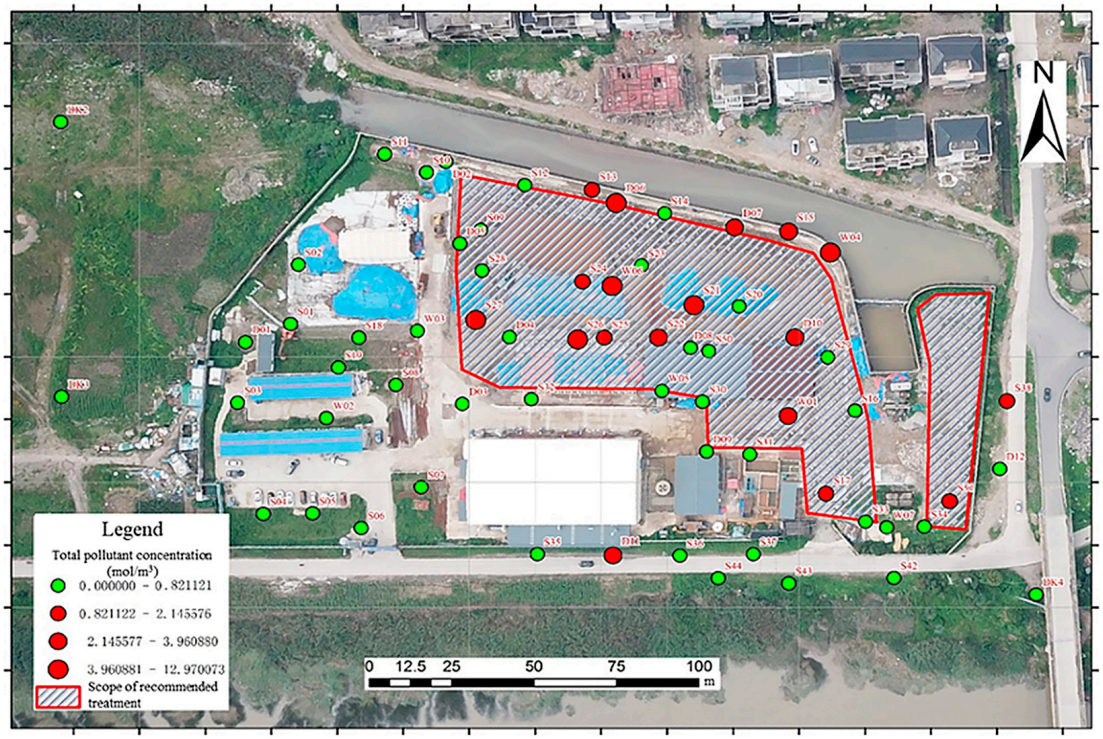

Figure 1. Distribution of contaminants at the site.

2.2. Geological Profile

The polluted site, a chemical enterprise in Zhejiang Province, is situated in a coastal plain terrain with relatively flat topography. Based on the exploration results, combined with the origin and properties of the foundation soil layers, as well as indoor experimental outcomes, the foundation bedrock can be divided into ten engineering geological units. From top to bottom, these geological units include unconsolidated fill, clay, silty clay, rounded gravel, clay, rounded gravel, fine-grained clay, clayey gravel with cohesion, gravelly silt with cohesion, and highly weathered tuffaceous rock. After the initial site processing, the topsoil was excavated, resulting in a pit 3.9 m deep within the study area.

2.3. Groundwater Conditions

Above the groundwater Table, there is an unsaturated zone with a thickness ranging from 0.5 to 1.7 m in the unconsolidated fill and fine-grained clay layers. Due to the excavation of the pit, there is virtually no unsaturated zone in the study area. Below the groundwater Table, the layers of silty clay, rounded gravel, clay, and rounded gravel

exhibit a complex distribution and high heterogeneity, constituting the aquifer system. The lower layers of fine-grained clay, clayey gravel with cohesion, gravelly silt with cohesion, and highly weathered tuffaceous rock are characterized by very low permeability due to cohesive soils, predominantly functioning as confining layers with relatively low hydraulic conductivity.

3. Software and Methodology

3.1. Software

COMSOL Multiphysics is a powerful multiphysics simulation software developed by COMSOL AB, widely used in various fields such as engineering, scientific research, and education. It supports the simulation of coupled multiphysics phenomena, including but not limited to fluid dynamics, heat transfer, and electromagnetism, as well as more advanced custom equations, such as the coupling of Groundwater Contaminant Transport with Bacterial Chemotaxis movement in this study. This coupling simulation allows researchers to analyze the transport behavior of contaminants in groundwater and the response of bacteria to these contaminants. COMSOL provides a graphical user interface, advanced solvers, parameterized modeling, rich post-processing tools, and support for APIs and scripting. Its modular design and intuitive interface further enhance the software's flexibility and user-friendliness. These features enable engineers and researchers to efficiently design and optimize complex systems at the design stage, predict product performance, and save time and cost in the research and development process.

3.2. Groundwater Contaminant Transport Mathematical Model

Contaminants in the subsurface are present on the surfaces of geological particles and within the pore spaces of geological formations, and they move with the flow of groundwater. Contaminants migrate with the natural water cycle in the subsurface and are influenced by human activities such as pumping. Additionally, dissolved contaminants in groundwater undergo diffusion due to concentration differences between different regions. The sorption and desorption of contaminants also occur between groundwater and soil due to concentration disparities.

We have simulated the dry winter season, accounting for the effects of moisture evaporation. In layers 1—silty clay and 2—rounded gravel, which are in contact with the air, we employ the Richards equation to simulate the flow of unsaturated groundwater. In layers 3—clay and 4—rounded gravel, as well as the aquifer with relative confining properties, Darcy's Law is commonly used in COMSOL software to describe this flow process.

Darcy's law is a fundamental equation for describing fluid flow in porous media, derived from experiments involving water flow through sand layers, and holds significant importance in hydrogeology [22]. It outlines the principles of fluid flow in porous media as follows:

$$\mathrm{q} = -\frac{k}{\mu L}\Delta p, \tag{1}$$

This equation defines the absolute permeability for describing single-phase flow. The symbols in the equation include q (flow rate, units: m/s), k (permeability, units: m^2), μ (fluid viscosity, units: Pa·s), L (length of the rock sample, units: m), and Δp (pressure difference between the left and right ends, units: Pa). It exhibits high reliability when dealing with conventional saturated flow.

Darcy's Law is an empirical law that mathematically combines various factors influencing fluid flow in porous media. It is primarily applicable to laminar flow conditions, where groundwater flow in fine-grained or coarse-grained sediments is predominantly laminar. Darcy's Law finds extensive application in groundwater flow and petroleum engineering, particularly when addressing saturated flow problems.

For formations above the water Table, the formation is unsaturated with both water and gas in the formation. This is usually described in COMSOL using the Richards equation.

The Richards equation is used to describe the movement of water in unsaturated soils and was proposed by Lorenzo A. Richards in 1931 [23]. This equation builds upon Darcy's Law but is suitable for unsaturated flow situations. It involves parameters such as hydraulic conductivity (K), pressure head (h), elevation (z), volumetric water content (θ), time (t), and others. The equation describes the variation in volumetric water content with time and expresses the rate of change of saturation by considering variations in the inflow and outflow fluxes.

$$\frac{\partial \theta}{\partial t} = \frac{\partial}{\partial z}\left(K(\theta)\left(\frac{\partial h}{\partial z}\right) + 1\right), \tag{2}$$

In porous media, including both saturated and unsaturated conditions, it is essential to consider the processes of pollutant advection, diffusion, and adsorption simultaneously to perform accurate numerical simulations of pollutant transport. The advection–diffusion equation for pollutants describes the dissolution of pollutants in groundwater and their movement towards regions of lower concentrations in the presence of concentration gradients. The general form of this equation is expressed as follows [24]:

$$\frac{\partial c}{\partial t} = \nabla(\mathrm{D}\nabla \mathrm{c}) - \nabla(v\mathrm{c}) + \mathrm{R}, \tag{3}$$

In this context, 'c' represents the variable under investigation, which could be the concentration of a solute in the case of mass transfer or the temperature in the context of heat transfer. 'D' signifies the diffusion coefficient, where diffusion refers to the movement of particles in the case of mass transfer and thermal conduction in the case of heat transfer. 'v' represents the velocity field that arises during diffusion phenomena, and it is a function of both time and space. Given that this simulation is three-dimensional, 'v' encompasses components in the x, y, and z directions, as determined by Darcy's law and the Richards equation. 'R' denotes the source term for the chemical species involved, where $R > 0$ indicates a chemical reaction generating more of the species, and $R < 0$ indicates a chemical reaction consuming the species.

Freundlich adsorption isotherms are commonly used in COMSOL software to describe adsorption phenomena. The Freundlich adsorption isotherm is an empirical relationship that describes the quantity of gas adsorbed onto a solid surface as a function of gas pressure. A similar relationship holds for the concentration of a solute adsorbed onto a solid surface concerning the solute's concentration in the liquid phase.

The Freundlich adsorption isotherm can be mathematically represented in various forms [25], such as the following:

$$\frac{x}{m} = \mathrm{K}p^{1/n}, \tag{4}$$

$$\log\frac{x}{m} = \log\mathrm{K} + \frac{1}{n}\log p, \tag{5}$$

$$\frac{x}{m} = \mathrm{K}c^{1/n}, \tag{6}$$

$$\log\frac{x}{m} = \log\mathrm{K} + \frac{1}{n}\log c, \tag{7}$$

In the given expressions, x represents the mass of the adsorbed substance, m denotes the mass of the adsorbent, p stands for the equilibrium pressure of the adsorbate in the gas phase during experimentation, and c signifies the equilibrium concentration of the adsorbate when in contact with the dispersed solid phase (dissolved species/adsorbed species) in an aqueous solution. Both K and n are constants for the adsorbate and adsorbent at a given temperature. When the pressure is very high, i.e., when $1/n = 0$, the extent of adsorption becomes independent of pressure.

3.3. Bacterial Chemotaxis Model

To explore the feasibility of applying chemotactic bacteria in the industrial plant area, a numerical simulation was conducted, incorporating a bacterial concentration field to simulate bacterial chemotaxis. The free movement of bacteria is represented by an effective diffusion coefficient, while convection is determined by the flow velocity obtained from the flow field model. An additional chemotactic term is introduced to account for motion towards the gradient of the attractant concentration [26]. The term of bacterial chemotaxis is coupled to pollutant diffusion processes by customizing equations in COMSOL.

$$v_{Chx} = \frac{2}{3} v_b \tanh\left(\frac{\chi_0}{2v_b} \frac{K_c}{(K_c + a)^2} \frac{\partial a}{\partial x}\right), \tag{8}$$

$$v_{Chy} = \frac{2}{3} v_b \tanh\left(\frac{\chi_0}{2v_b} \frac{K_c}{(K_c + a)^2} \frac{\partial a}{\partial y}\right), \tag{9}$$

$$v_{Chz} = \frac{2}{3} v_b \tanh\left(\frac{\chi_0}{2v_b} \frac{K_c}{(K_c + a)^2} \frac{\partial a}{\partial z}\right), \tag{10}$$

In this context:

- "v_b" represents the bacterial free-swimming speed.
- "a" represents the attractant concentration.
- "χ_0" stands for the chemotaxis sensitivity coefficient, indicating the degree of response to the gradient of attractant concentration.
- "K_c" is the chemoreceptor's kinetic constant, related to the receptor saturation concentration.
- $\partial a/\partial x$, $\partial a/\partial y$, $\partial a/\partial z$ represent the gradients of the attractant concentration in the x, y, and z directions, respectively.

Bacterial chemotaxis velocity is directly proportional to the local gradient of attractant concentration and is also influenced by the bacterial chemotactic parameters.

4. Results and Discussion

4.1. Hydrogeological Model

The top soil layer of the treatment area was excavated on site to form a 2.3 m deep pit, and the excavated portion is shown in the left solid red line area in Figure 1. Based on the geologic profile information obtained from the on-site exploratory wells, layering can be performed using COMSOL's parametric surface function. Based on the engineering geological units of the foundation bedrock, the study area, from a depth of 2.3 m to 30 m below the pit, is divided into five layers. The stratigraphy is summarized in Figure 2. From top to bottom, these layers are 1—silty clay, 2—rounded gravel, 3—clay, 4—rounded gravel, and 5—aquifer with relative confining properties. Layers 1 to 4 constitute the aquifer, while the remaining layers below are conceptualized as aquifers with relative confining properties. The dashed circles in Figure 2 represent well locations, with Well 7 and Well 8 serving as injection wells, while the others are extraction wells. The wells have a diameter of 0.2 m and a depth of 14 m.

In this study, we employed a method involving homogeneous extraction wells and injection wells for the remediation of various categories of pollutants present in the soil and soil pores. Pollution elimination was achieved by injecting water into pressure-inlet wells and pumping water from eight surrounding wells. We utilized Darcy's law interface, with the central two wells designated as pressure inlets, maintaining a water column pressure of 5 m at the wellheads. We established an analytical function using COMSOL to account for boundary pressures in wells of varying heights.

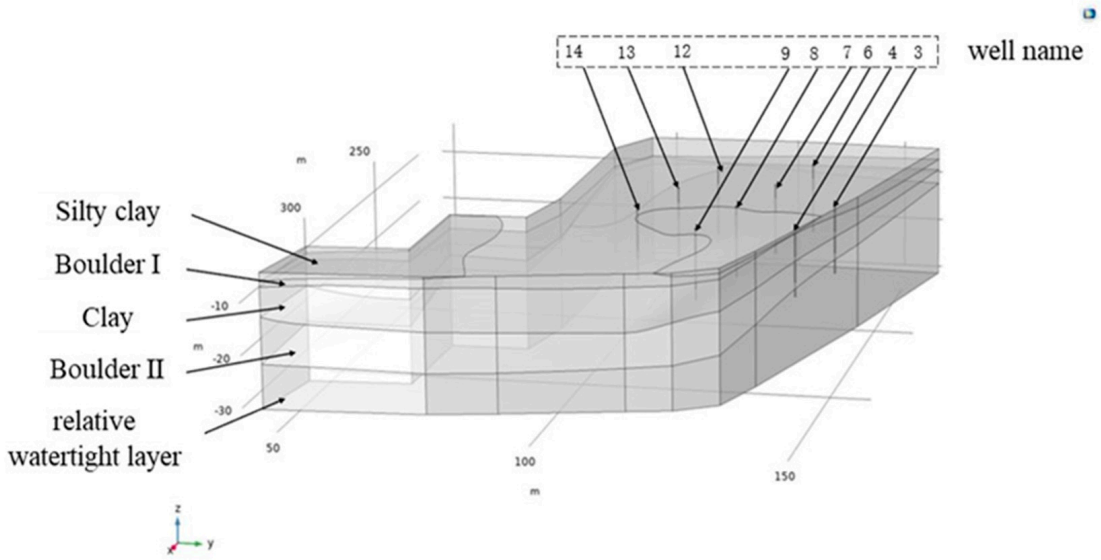

Figure 2. Stratigraphy and well locations.

Non-flow boundary conditions were set to simulate impermeable membranes and low-permeability rocks to prevent flow to the surroundings. The top interface represented the boundary between soil and water, and as there was no groundwater seeping to the surface, it was also set as a non-flow boundary. Initial conditions included the initialization of pore pressures, where locations with zero depth were considered to be in contact with the atmosphere, thus having pore pressure equal to atmospheric pressure. At different depths, pore pressure was approximately equal to static water pressure, and we used analytical functions to set these initial pressure values.

Since the testing period occurred during winter with lower precipitation and a lower groundwater Table, we set the soils in contact with the atmosphere in the excavation pit to have 95% variable saturation flow. Thus, the top two layers are described using Richard's equation, while the deeper ones are below the water level and are described using Darcy's law. Based on on-site testing data, we adjusted the porosity and permeability of different soil layers to account for seasonal variations and soil properties. The porosity and hydraulic conductivity of each layer of the site were provided by the Zhejiang Provincial Exploration Institute through exploratory wells, taking cores, and indoor experiments. For more detailed information, please refer to Table 1.

Table 1. Information on stratified soils.

Layer	Control Equation (Math.)	Porosity	Hydraulic Conductivity/m·s^{-1}
1	Richards equation	0.55	1.2×10^{-9}
2	Richards equation	0.55	2.03×10^{-4}
3	Darcy's law	0.55	5×10^{-9}
4	Darcy's law	0.55	5.25×10^{-4}
5	Darcy's law	0.412	5×10^{-10}

For the setting of initial values, an analysis was conducted summarizing the types and concentrations of pollutants measured in the on-site soil. It was found that the majority of pollutants consisted of volatile organic compound s(VOC) and semi-volatile organic compounds (SVOC), as well as extractable petroleum hydrocarbons (EPH). By organizing this information, the distribution of pollutants with different diffusion properties in the well field coordinate system was obtained. Interpolation functions for pollutant initial values were defined using COMSOL.

The primary substance exchange in the process of pollutant removal occurs between groundwater and subsurface soil, as well as the diffusion of pollutants between ground-

water driven by differences in pollutant concentrations. Therefore, in this interface, both diffusion and adsorption processes were considered. Some researchers [20] have extensively studied the adsorption behavior of petroleum pollutants in different soils and provided correlation coefficients for the Freundlich isotherm adsorption model. Based on experimental studies and numerical simulations from the literature, the Freundlich constant was taken as 3.63×10^{-3} mol/Kg, and the Freundlich exponent was set to 1.09.

To select the diffusion coefficient, D, parametric scans were performed using the concentration test data of pollutants at different time points at the same well location. A series of values for the diffusion coefficient, D, were set for parametric scan calculations. During this step, different pollutants were calculated separately, and based on actual on-site experiments, only extraction well No. 6 and injection well No. 7 were activated, with a simulation time of 55 days. The value of the diffusion coefficient, D, was continuously changed, and the model was calculated, with all model results saved. After the calculations were completed, the concentration of pollutants at the bottom of well No. 6 was calculated using the derived value function. The size of this value for different diffusion coefficients was observed and compared with the measured values. Utilizing the principle of binary search, optimization was performed continuously until the value of the diffusion coefficient, D, matched the measured pollutant concentration. The parameter values optimized based on on-site experimental data are shown in Table 2.

Table 2. Optimized parameter values.

Pollutant Type	Diffusion Coefficient/$m^2 \cdot s^{-1}$	Adsorption Constant/$mol \cdot kg^{-1}$	Adsorption Index
VOC	2×10^{-5}	3.63×10^{-3}	1.09
SVOC	1.3×10^{-4}	3.63×10^{-3}	1.09
EPH	2.3×10^{-3}	3.63×10^{-3}	1.09

4.2. Pollutant Distribution

In accordance with the site remediation strategy, the next step in the remediation process involves the injection and extraction treatment by opening all wells. Three types of pollutants are considered at the interface of dilute substances, with the initial pollutant distribution data and diffusion and adsorption parameters incorporated into the overall model. The simulation spans a duration of 55 days.

After 55 days of remediation, the total amount of VOC decreased by 16.6%, reducing from 20.768 mol to 17.316 mol. The total amount of SVOC decreased by 23%, dropping from 2.9869 mol to 2.3 mol. Additionally, the total amount of EPH decreased by 42.5%, decreasing from 5.1552 mol to 2.9658 mol.

The changes in pollutant concentrations from day zero to day 55 are presented in Figure 3.

From Figure 3, it is evident that different types of pollutants exhibit distinct spatial distributions at day zero. Volatile and SVOC are primarily distributed to the west of the remediation area, which is attributed to the previous production activities in this region, resulting in the release of volatile chemicals. In contrast, EPH exhibit a relatively even distribution, present in both the central and northern parts of the factory area due to leakage from the factory's raw materials.

Furthermore, Figure 3 illustrates that during the initial injection and extraction phases, pollutants tend to distribute more uniformly. This is because the external flow field disrupts the original equilibrium of pollutants, causing them to diffuse from areas of high concentrations to areas of lower concentrations. With increasing treatment times, the pollutants are removed from the extraction wells, desorb from the soil under the influence of the external flow and concentration fields, dissolve into groundwater, and are transported away by water flow. However, in the later stages of the extraction process, pollutants tend to approach the boundary region due to the difficulty of the flow field reaching the boundary. Pollutants that desorb in the soil near the boundary are reabsorbed. While

pollutant removal is more effective around the injection wells, it is not complete due to soil adsorption. To enhance removal, higher injection pressure or the use of surfactants can be considered.

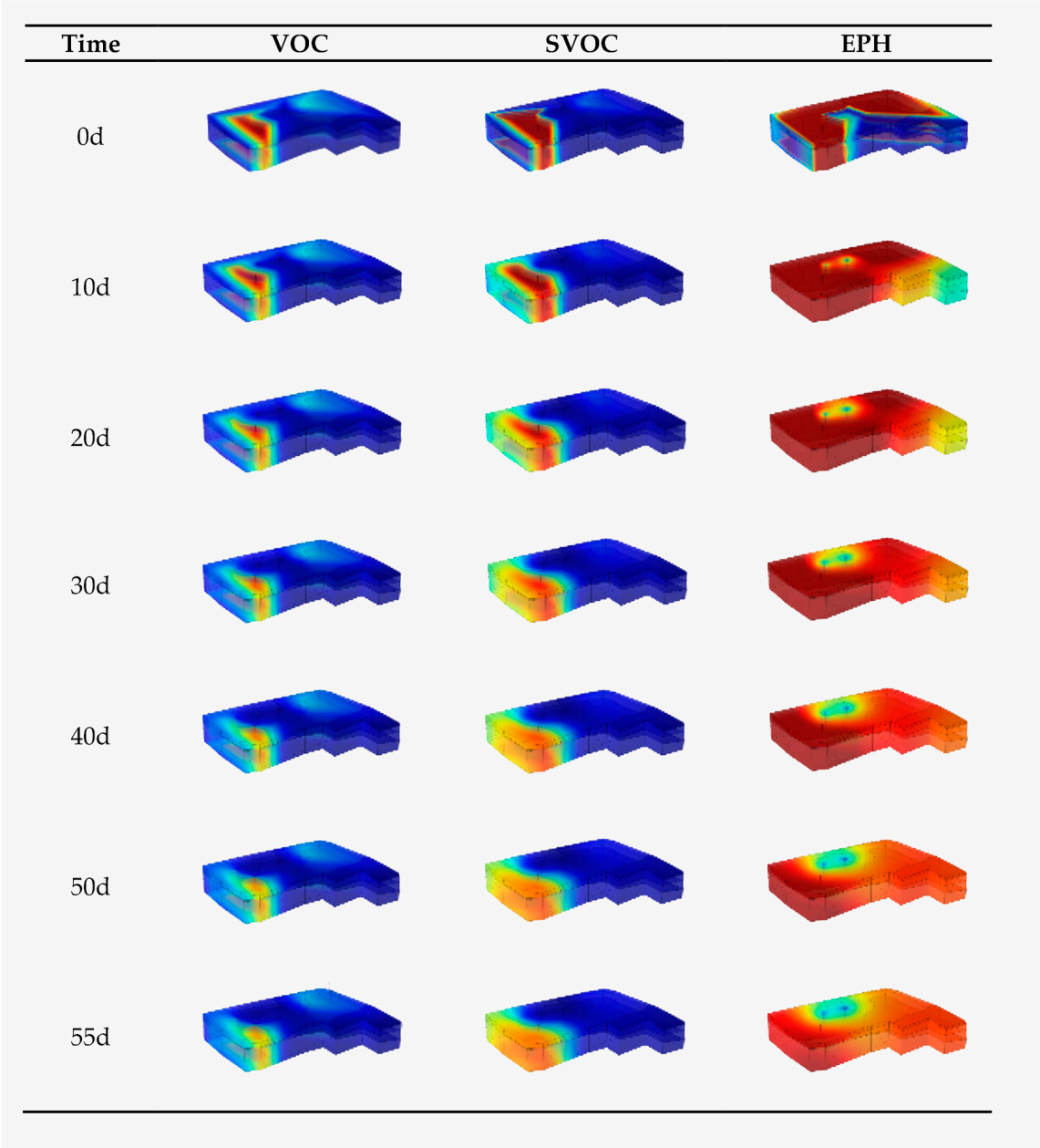

Figure 3. Changes in pollutant concentrations.

In this simulation, non-aqueous phase pollutants are not considered; all pollutants in the model are either dissolved in water or adsorbed onto soil. The addition of surfactants can reduce soil adsorption, leading to better remediation results. For this numerical simulation, the effect of adding surfactants is achieved by altering the Freundlich adsorption constant.

The remediation results after 55 days for different Freundlich adsorption constants are presented in Figure 4.

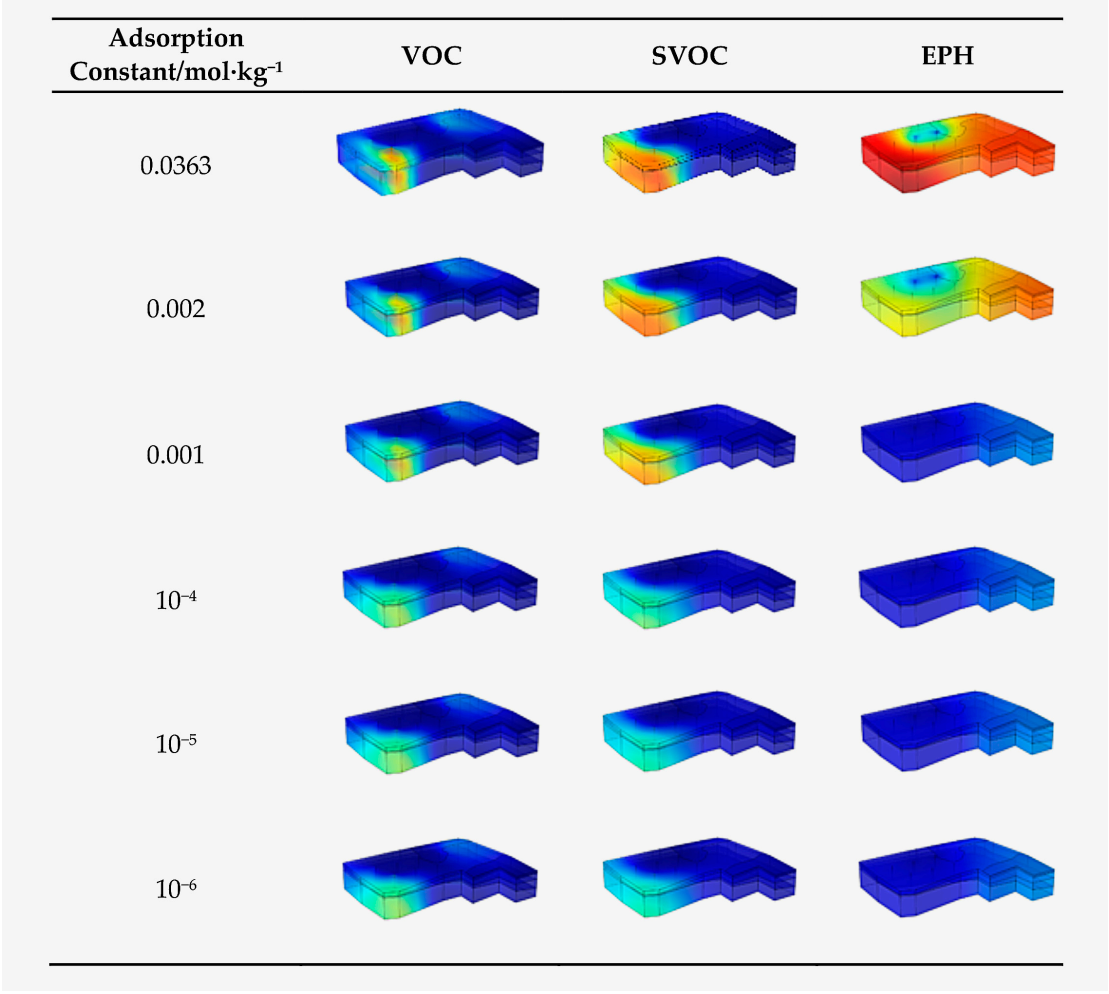

Figure 4. Remediation results for different Freundlich adsorption constants after 55 days.

From Figure 4, we gain a deeper understanding of the intricate relationship between the Freundlich adsorption constant and soil remediation efficiency. This relationship does not adhere to the simplistic principle of "the smaller, the better" but rather reveals a more nuanced dynamic equilibrium. The magnitude of the Freundlich adsorption constant directly influences the adsorption capacity of pollutants in the soil, where a smaller constant implies a stronger adsorption capacity under given conditions. However, this enhanced adsorption capacity does not always translate directly into more effective remediation, as an increase in the surfactant concentration, while increasing the solubility of pollutants, may also lead to increased costs and other potential environmental risks when the concentration is excessively high.

Notably, when the Freundlich adsorption constant is reduced below 0.001 mol/Kg, we observe that further decreases in the constant contribute minimally to the improvement of remediation effects. This is clearly demonstrated in Figures 5–7, which describe the relationship between the total concentrations of different pollutants and the Freundlich adsorption constant. These diagrams reveal a similar trend for three types of pollutants—VOC, SVOC, and PAH—in response to changes in the adsorption constant. Initially, a relatively small reduction in the adsorption constant leads to a significant enhancement in remediation effects, but when the adsorption constant drops below 10^{-5}, the total concentrations of pollutants follow a similar trend over time, indicating that further reductions in the adsorption constant do not significantly enhance remediation. This pattern suggests that in the remediation process, we need to find an optimal value for the adsorption constant to maximize cost-effectiveness and environmental benefits.

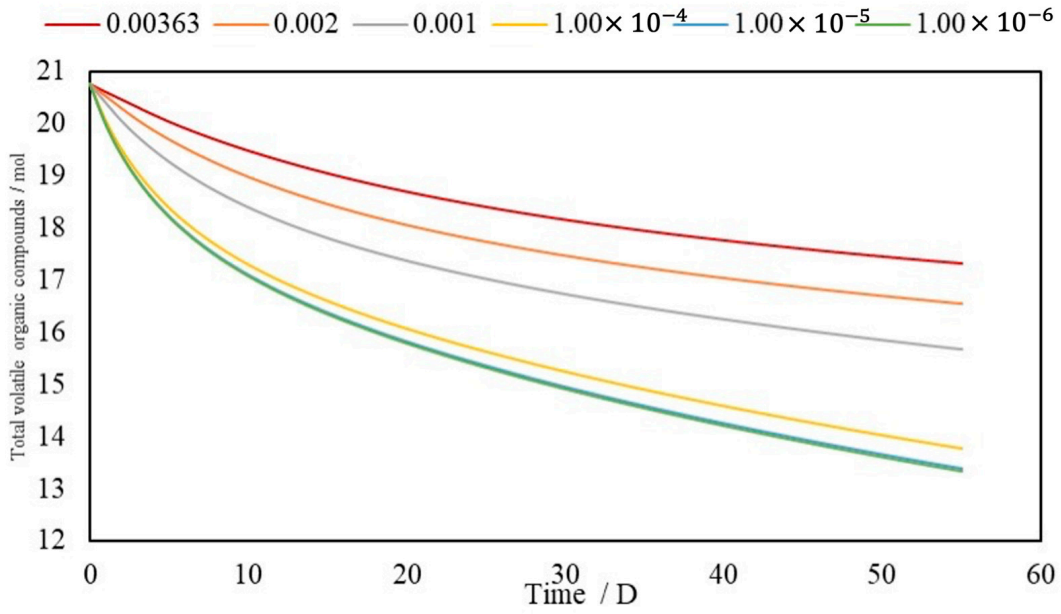

Figure 5. Relationship between total VOC and adsorption constant.

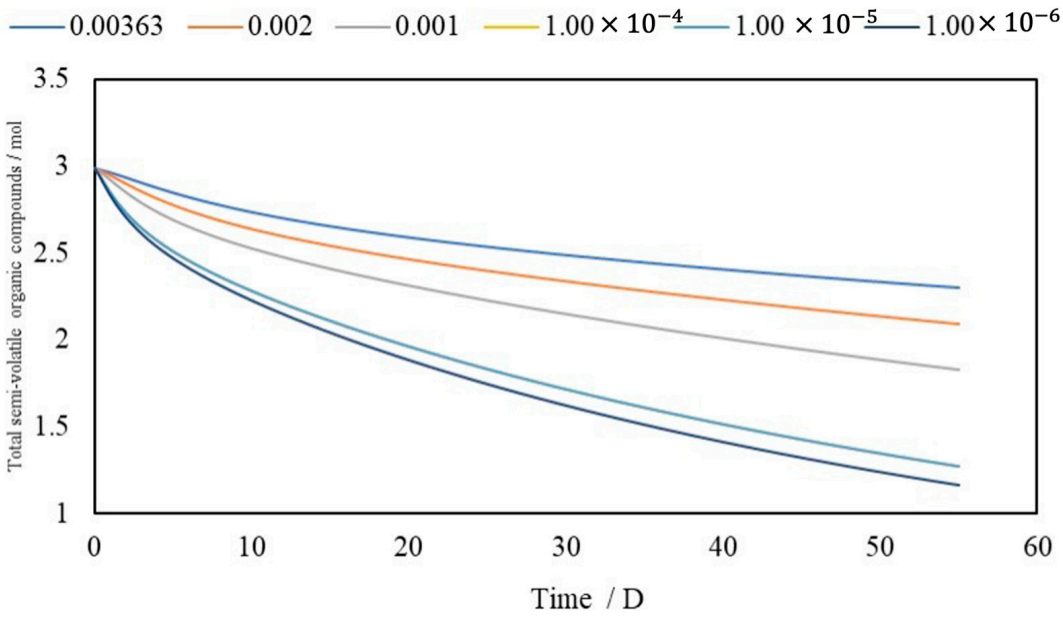

Figure 6. Relationship between total SVOC and adsorption constant.

After a 55-day remediation period, the final content of VOC in relation to different adsorption constants further confirms this point. The gradual reduction in the adsorption constant initially leads to an enhancement of remediation effects, but when the adsorption constant falls below a certain threshold, this enhancement begins to weaken. According to the analysis in Figure 8, we find that the optimal range for the adsorption constant is between 0.001 and 0.0001, where it can effectively promote the removal of pollutants while avoiding the weakening of remediation effects due to an overly small adsorption constant.

Therefore, when designing soil remediation strategies, we must not only consider the optimal balance point of the adsorption constant but also the sustainability of long-term remediation effects. This means finding a balance between improving pollutant removal efficiency and controlling costs while ensuring that the remediation process does not impose new burdens on the environment.

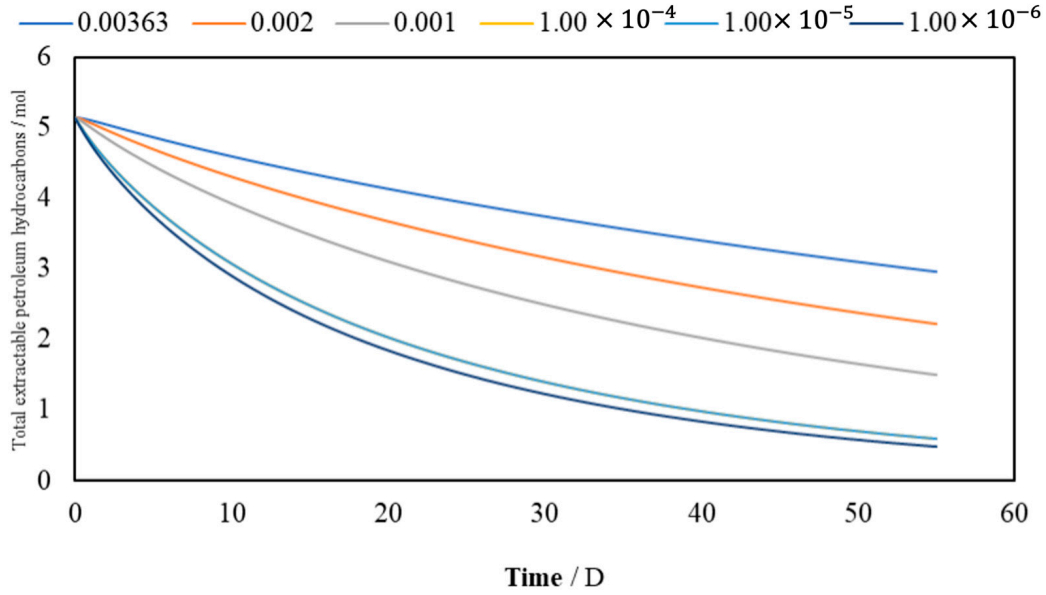

Figure 7. Relationship between total EPH and adsorption constant.

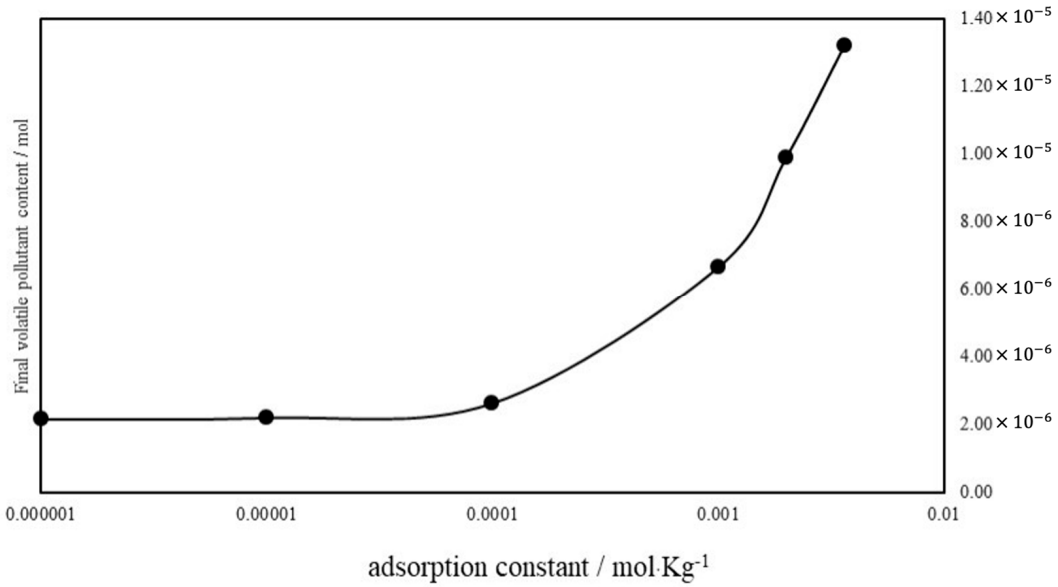

Figure 8. Final volatile pollutant content at different adsorption constants.

4.3. Microbial Remediation with Chemotaxis Optimization

In the context of groundwater pollution by petroleum contaminants resulting from a chemical factory's leakage, the use of chemotactic bacteria for bioremediation proves more effective compared to traditional physical methods, such as hydraulic flushing. This efficacy stems from the inherent characteristics of petroleum contaminants, including their tendency to adhere to soil and their low volatility, making them less susceptible to removal by hydraulic flushing. Instead, they often become trapped in areas of lower groundwater permeability, making it challenging to remove them solely through water flow. Moreover, this can lead to the further spread of pollutants, exacerbating the contamination. In contrast, the application of chemotactic bacteria (e.g., Pseudomonas putida) in bioremediation can overcome these limitations.

First, chemotactic bacteria have the capability to directly degrade and absorb petroleum contaminants. Second, due to their chemotaxis, they can actively move towards areas with higher pollutant concentrations, attracted to low-permeability zones where they degrade

pollutants that are difficult to remove through hydraulic flushing. Lastly, as pollutants are locally degraded, bacterial populations increase, continuously enhancing the bioremediation capacity of the contaminated site. Thus, compared to traditional physical methods, chemotactic bacteria can achieve more efficient and controllable in situ pollutant degradation, mitigating spread, and are a more suitable bioremediation approach in such scenarios.

To attract chemotactic bacteria, the attractant is set as VOC with a concentration of 1 mol/m^3, causing chemotactic bacteria to migrate with the injected water. After one year of extraction simulation, the distribution of chemotactic and non-chemotactic bacteria is illustrated in Figure 9. The results from the figure show that non-chemotactic bacteria predominantly accumulate near the injection well and are mainly present in high-permeability areas. Conversely, chemotactic bacteria exhibit a wider distribution due to their attraction to pollutants.

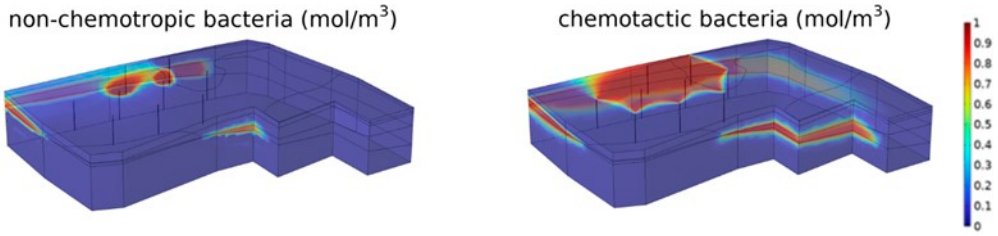

Figure 9. Distribution of non-chemotactic and chemotactic bacteria after one year of water injection.

A cross-sectional plane is taken near the injection well, as depicted in Figure 10. Bacterial concentrations and streamlines are plotted on this plane, as shown in Figure 11. The total concentration of chemotactic bacteria on this plane is 356.8 mol, while non-chemotactic bacteria have a concentration of 278.58 mol. Non-chemotactic bacteria primarily disperse along the direction of streamlines, while the distribution of chemotactic bacteria is less correlated with the flow field.

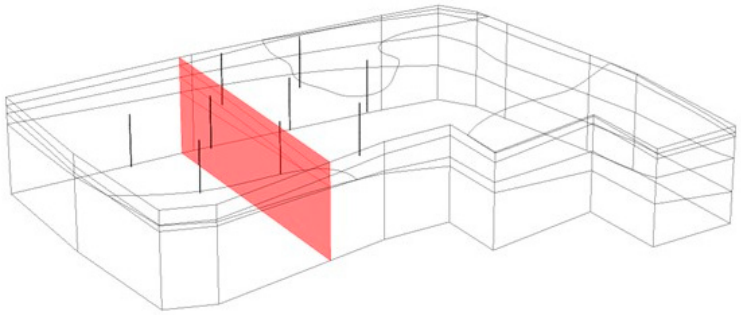

Figure 10. Selected research plane.

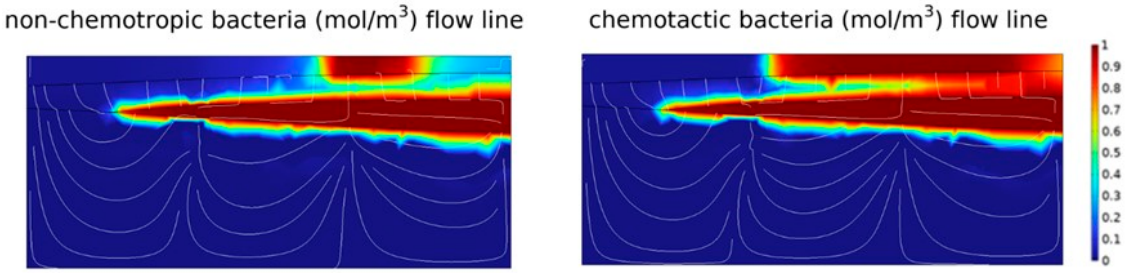

Figure 11. Concentration distribution of non-chemotactic and chemotactic bacteria on the cross-section plane with streamlines.

Observations indicate that chemotactic bacteria do not exhibit strong chemotaxis in the direction of VOC concentration gradients. This is due to the initially high bacterial

growth concentration set, which leads to decreased pollutant concentrations after water extraction. For lower pollutant concentrations, chemotactic bacteria become less active.

In practical remediation work, the removal of low-concentration pollutants is equally important. Therefore, reducing the optimal growth concentration for chemotactic bacteria is necessary. The resulting cross-sectional image is shown in Figure 12a. Reducing the optimal growth concentration for chemotactic bacteria does enhance chemotaxis to some extent. However, the effect is not significant due to the strong heterogeneity of the soil, resulting in minimal bacterial movement into low-permeability areas. Additionally, chemotactic bacteria with reduced optimal growth concentrations exhibit less activity when pollutant concentrations are initially high, which limits their spread.

To address this issue, genetic engineering can be employed to enhance chemotactic bacteria. This can involve increasing their chemotaxis, making them more inclined to move towards pollutants. Additionally, they can be engineered to undergo rapid mutations, facilitating their adaptation to the optimal growth concentration based on pollutant concentrations in groundwater. In the model, increasing the chemotactic sensitivity coefficient χ_0 and setting the chemoreceptor kinetics constant K_c as a linearly decreasing function of time produces the cross-sectional image shown in Figure 12b. This means that during the bioremediation process, the bacteria can quickly adapt to the continuously decreasing VOC concentrations, rather than simply cultivating bacteria with the optimal growth concentration set for low concentrations of VOC. This results in a significant increase in the range of chemotactic bacteria along the pollutant concentration gradient. The total concentration of chemotactic bacteria on this cross-section reaches 428.21 mol. After extraction is stopped, chemotactic bacteria, both enhanced and non-enhanced, undergo ten years of free diffusion, yielding the cross-sectional images depicted in Figure 12c,d, respectively. In the case of enhanced chemotactic bacteria, there is a substantial presence in low-permeability areas, with a total concentration of 787.15 mol, significantly higher than the 368.24 mol observed for non-enhanced chemotactic bacteria.

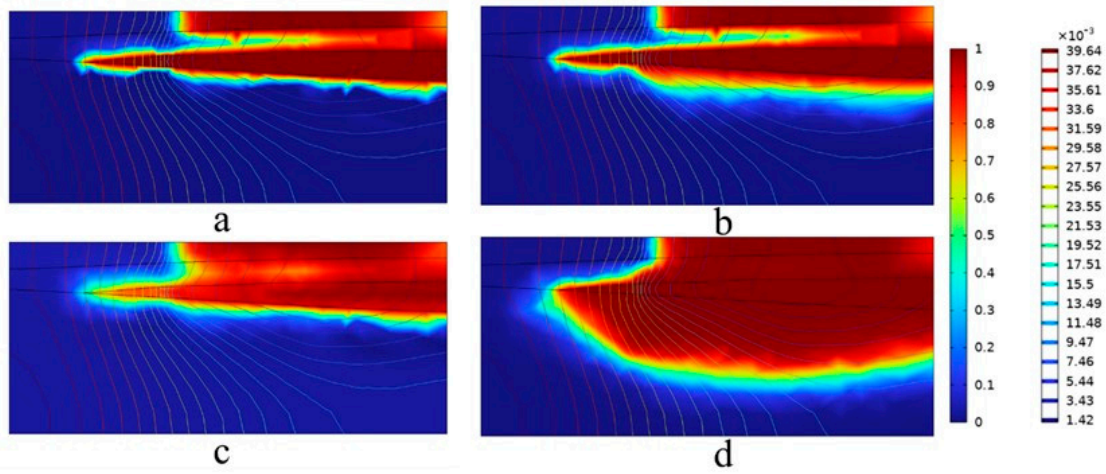

Figure 12. Concentration of chemotactic bacteria (cloud plot) vs. concentration of VOC (contours). (**a**) Chemotactic bacteria with reduced suitable growth concentration after one year's time. (**b**) Chemotactic bacteria intensified after one year's time. (**c**) Chemotactic bacteria with reduced suitable growth concentrations after ten years' time. (**d**) Chemotactic bacteria intensified after ten years' time.

A profile line is taken in the low-permeability area on the cross-section. The concentrations of VOC and chemotactic bacteria are plotted along this line. Figure 13 illustrates the concentrations of VOC and chemotactic bacteria after one year of water injection, while Figure 14 shows the concentrations after ten years of bacterial free diffusion. The black line represents the concentration of VOC, with pollutant concentrations ranging from 0.005 mol/m^3 to 0.04 mol/m^3, indicating a large concentration span. The red line represents

chemotactic bacteria that have not been selectively cultivated, the green line represents chemotactic bacteria selectively cultivated for low concentrations of VOC, and the blue line represents the enhanced chemotactic bacteria, as previously described, which are designed to quickly adapt to the decreasing concentrations of VOC. Following one year of injection, the concentration of enhanced chemotactic bacteria in the low-permeability zone is significantly higher than that of the other two chemotactic bacteria types. Although the chemotactic bacteria optimized for lower-concentration VOC perform slightly better than the original chemotactic bacteria, the effect is not substantial. Although the former have been optimized for low concentrations of VOCs and are initially active in the high-permeability area with high VOC concentrations when injected with water, the bacterial activity is not high in the early stages of treatment. The latter, however, show a lack of sensitivity to low concentrations of VOC, resulting in decreased bacterial activity in the later stages of the treatment process. After ten years of bacterial free movement, enhanced chemotactic bacteria exhibit a clear trend towards areas with higher VOC concentrations. The efficacy of the other two non-enhanced bacteria types in chemotaxis within the low-permeability area remains limited. This fully demonstrates that in the process of the engineering application of chemotactic bacteria, for pollutants that are difficult to deal with in low-permeability areas, the focus should be on enhancing the bacteria's ability to quickly adapt to the constantly changing pollutant concentrations.

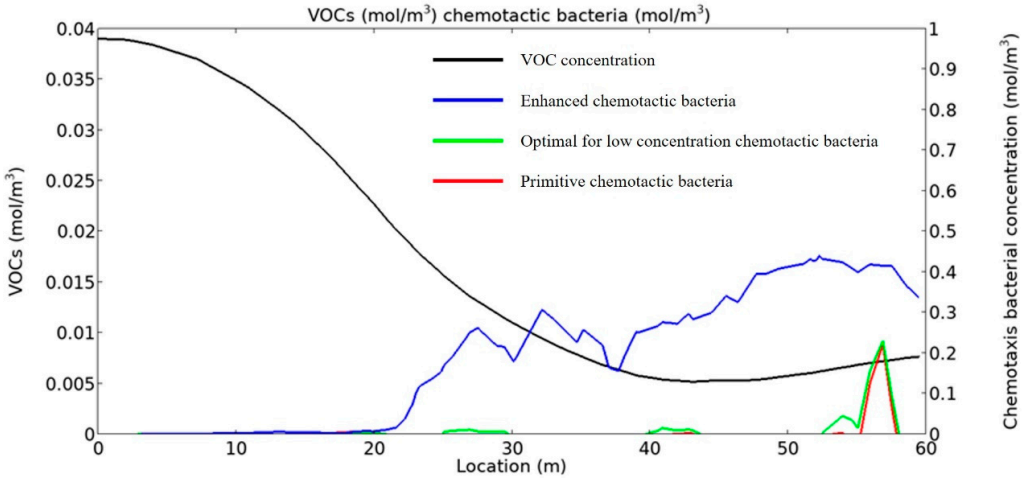

Figure 13. Concentration of VOC and chemotactic bacteria after one year of water injection.

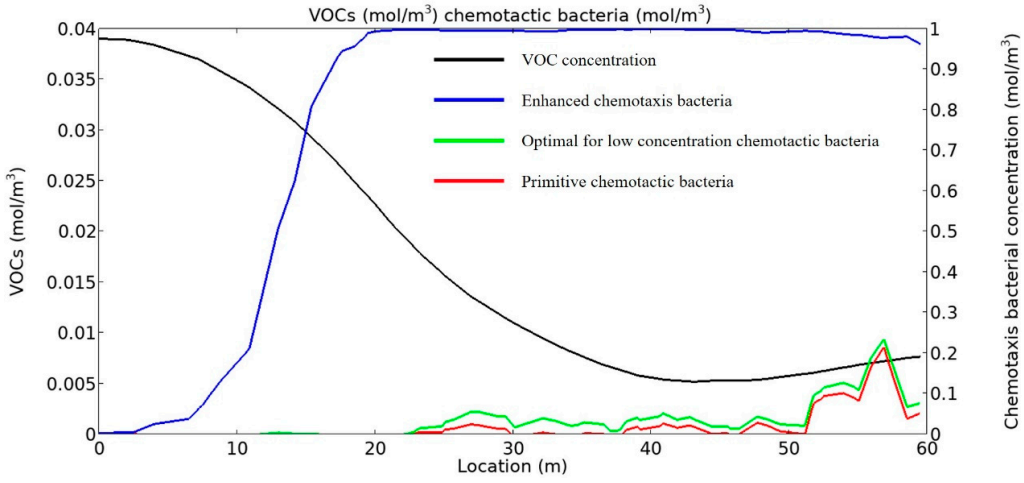

Figure 14. Concentration of VOC and chemotactic bacteria after ten years of bacterial random motility.

5. Conclusions

In this study, we conducted a comprehensive analysis of groundwater pollutant transport models, integrating the innovative application of bacterial chemotaxis to enhance the efficacy of groundwater remediation strategies. Groundwater contamination poses a significant and widespread environmental challenge, where conventional treatment methods have demonstrated limitations. Our findings underscore the significance of tailoring remediation approaches to the specific characteristics of each site, emphasizing the necessity for a multifaceted and interdisciplinary strategy. The numerical results indicate that chemotactic bacteria, which can rapidly adapt as the pollutant concentration decreases, have seen a 112% increase in concentration in the low-permeability area. The integration of genetic engineering offers a promising avenue for optimizing bacterial performance, potentially augmenting their chemotactic capabilities and resilience in diverse environmental conditions.

Moreover, we propose that a holistic approach, in the context of this research, involves not only the genetic enhancement of bacteria but also the synergistic application of chemotactic principles alongside other treatment modalities. The numerical results suggest that the use of some traditional remediation methods, such as surfactants, can increase the extent of impact on low-permeability areas, which will be beneficial to bioremediation.

With the increasing amount of research currently being conducted, chemotactic bacterial remediation is hopeful to stand out as a key component of environmental restoration efforts in the future. Especially for monocyclic or dicyclic aromatic hydrocarbons, due to their higher solubility in water, such pollutants buried in low-permeability areas can continuously dissolve in groundwater, posing a significant threat to human health. However, bacteria have a considerable decomposition efficiency for these types of pollutants. This method holds the promise of significantly mitigating the impact of contamination, leading to the restoration of cleaner and safer groundwater resources. The envisioned outcome is a sustainable and enduring solution for environmental recovery, one that integrates scientific innovation with ecological stewardship. This study only considered the chemotaxis of chemotactic bacteria, which is only one of the important indicators of chemotactic bacterial remediation, and in real life, it will involve many other aspects such as bacterial colonization and the decomposition of pollutants. Therefore, more research is needed in this area in the future.

Author Contributions: For the research article, the following contributions have been made by the authors: Conceptualization, S.C. and H.Z.; Methodology, S.C.; Software, X.W.; Validation, H.Z., X.W. and X.Z.; Formal analysis, S.C.; Investigation, X.Z.; Resources, H.Z.; Data curation, X.W.; Writing—original draft preparation, S.C.; Writing—review and editing, X.Z.; Visualization, X.W.; Supervision, T.L.; Project administration, H.Z. and T.L.; Funding acquisition, H.Z. All authors have read and agreed to the published version of the manuscript.

Funding: This research was funded by the Shandong Provincial Natural Science Foundation [grant number ZR2021ME108, ZX20220090, ZR2021JQ18], the Program of Nanjing Institute of Environmental Sciences, Ministry of Ecology and Environment: Integration of Ecological and Environmental Protection in Yangtze River Delta [grant number ZX2022QT047], and the Open Foundation of State Environmental Protection Key Laboratory of Soil Environmental Management and Pollution Control [grant number SEMPC2023002].

Institutional Review Board Statement: Not applicable.

Informed Consent Statement: Not applicable.

Data Availability Statement: Restrictions apply to the availability of these data. The data were obtained from the Program of Nanjing Institute of Environmental Sciences, Ministry of Ecology and Environment, and are available from the corresponding author with the permission of the third party.

Conflicts of Interest: The authors declare no conflicts of interest.

References

1. Wang, S.; Xu, Y.; Lin, Z.; Zhang, J.; Norbu, N.; Liu, W. The Harm of Petroleum-Polluted Soil and Its Remediation Research. *AIP Conf. Proc.* **2017**, *1864*, 020222. [CrossRef]
2. Zheng, J.; Fu, Y.; Song, Q.; Xie, J.; Lin, S.; Liang, R. Advances in the bioaugmentation-assisted remediation of petroleum contaminated soil. *Sheng Wu Gong Cheng Xue Bao=Chin. J. Biotechnol.* **2021**, *37*, 3622–3635. [CrossRef]
3. Lu, M.; Zhang, Z.; Qiao, W.; Guan, Y.; Xiao, M.; Peng, C. Removal of Residual Contaminants in Petroleum-Contaminated Soil by Fenton-like Oxidation. *J. Hazard. Mater.* **2010**, *179*, 604–611. [CrossRef] [PubMed]
4. Wang, X.; Ren, L.; Long, T.; Geng, C.; Tian, X. Migration and Remediation of Organic Liquid Pollutants in Porous Soils and Sedimentary Rocks: A Review. *Environ. Chem. Lett.* **2023**, *21*, 479–496. [CrossRef]
5. Luo, Y.M. Current Research and Development in Soil Remediation Technologies. *Prog. Chem.* **2009**, *21*, 558–565.
6. Zhao, X.Y.; Tan, W.B.; Dang, Q.L.; Li, R.F.; Xi, B.D. Enhanced Biotic Contributions to the Dechlorination of Pentachlorophenol by Humus Respiration from Different Compostable Environments. *Chem. Eng. J.* **2019**, *361*, 1565–1575. [CrossRef]
7. Zheng, L.; Long, T.; Lin, Y.; Yu, C.; Liu, Y.; Zhu, X. Biolog-ECO Analysis of Microbial Community Functional Diversity in Organochlorine Contaminated Soil. *Chin. J. Appl. Environ. Biol.* **2013**, *19*, 759–765. [CrossRef]
8. Zhou, B.H.; Yuan, R.F.; Shi, C.H.; Yu, L.Y.; Gu, J.N.; Zhang, C.L. Biodegradation of Geosmin in Drinking Water by Novel Bacteria Isolated from Biologically Active Carbon. *J. Environ. Sci.* **2011**, *23*, 816–823. [CrossRef]
9. Wang, Q.; Yang, Z.; Yin, L.; Song, X.; Wei, C.; Li, Y.; Zhai, W. Bibliometric analysis on bioremediation of organic contaminated soil and groundwater based on Web of Science database. *Sheng Wu Gong Cheng Xue Bao=Chin. J. Biotechnol.* **2021**, *37*, 3549–3564. [CrossRef]
10. Li, H.L.; Boufadel, M.C. Long-Term Persistence of Oil from the Exxon Valdez Spill in Two-Layer Beaches. *Nat. Geosci.* **2010**, *3*, 96–99. [CrossRef]
11. Gao, B.; Wang, X.; Ford, R.M. Chemotaxis along Local Chemical Gradients Enhanced Bacteria Dispersion and PAH Bioavailability in a Heterogenous Porous Medium. *Sci. Total Environ.* **2023**, *859*, 160004. [CrossRef]
12. Parales, R.E.; Ditty, J.L.; Harwood, C.S. Toluene-Degrading Bacteria Are Chemotactic towards the Environmental Pollutants Benzene, Toluene, and Trichloroethylene. *Appl. Environ. Microbiol.* **2000**, *66*, 4098–4104. Available online: http://Aem.Asm.Org/ (accessed on 13 November 2012). [CrossRef] [PubMed]
13. Pedit, J.A.; Marx, R.B.; Miller, C.T.; Aitken, M.D. Quantitative Analysis of Experiments on Bacterial Chemotaxis to Naphthalene. *Biotechnol. Bioeng.* **2002**, *78*, 626–634. [CrossRef] [PubMed]
14. Zhao, F.; Liu, H.; Wang, S.; Niu, G.; Zhou, N. Chemotaxis of Pseudomonas sp. Strain ZWL73 to 4-chloronitrobenzene and various aromatic compounds. *J. Zhejiang Univ.* **2004**, *30*, 624–627.
15. Qiao, C.; Ren, L.; Jia, Y.; Fan, S.; Wang, J.; Yan, Y. Chemotaxis of Arthrobacter sp. CN2 towards p-nitrophenol. *J. Agro-Environ. Sci.* **2016**, *35*, 1945–1952.
16. Strobel, K.L.; McGowan, S.; Bauer, R.D.; Griebler, C.; Liu, J.; Ford, R.M. Chemotaxis Increases Vertical Migration and Apparent Transverse Dispersion of Bacteria in a Bench-Scale Microcosm. *Biotechnol. Bioeng.* **2011**, *108*, 2070–2077. [CrossRef]
17. Xie, W.; Ren, B.; Hursthouse, A.S.; Wang, Z.; Luo, X. Simulation of Manganese Transport in Groundwater Using Visual MODFLOW: A Case Study from Xiangtan Manganese Ore Area in Central China. *Pol. J. Environ. Stud.* **2021**, *30*, 1409–1420. [CrossRef]
18. Alexander, A.C.; Ndambuki, J.M. Optimal Design of Groundwater Pollution Management Systems for a Decanting Contaminated Site: A Simulation-Optimization Approach. *Groundw. Sustain. Dev.* **2021**, *15*, 100664. [CrossRef]
19. Pongritsakda, T.; Nakamura, K.; Wang, J.; Watanabe, N.; Komai, T. Prediction and Remediation of Groundwater Pollution in a Dynamic and Complex Hydrologic Environment of an Illegal Waste Dumping Site. *Appl. Sci.* **2021**, *11*, 9229. [CrossRef]
20. Shakeri, R.; Nassery, H.R.; Ebadi, T. Numerical Modeling of Groundwater Flow and Nitrate Transport Using MODFLOW and MT3DMS in the Karaj Alluvial Aquifer, Iran. *Env. Monit Assess* **2022**, *195*, 242. [CrossRef]
21. El-Aassar, A.-H.; Hagagg, K.; Hussien, R.; Oterkus, S.; Oterkus, E. Integration of Groundwater Vulnerability with Contaminants Transport Modeling in Unsaturated Zone, Case Study El-Sharqia, Egypt. *Env. Monit Assess* **2023**, *195*, 722. [CrossRef]
22. Zhong, W.; Tian, Z.; Wang, T. Regularity of Gas Leakage from Underground Chemical Explosions Based on Dimensional Analysis and Darcy's Law. *Chin. J. Comput. Phys.* **2019**, *36*, 449–456.
23. Jones, W.F. A Numerical Analysis of Richards' Equation for Unsaturated Porous Media Flow. Ph.D. Thesis, Clemson University, Clemson, SC, USA, 1994.
24. Cui, S.; Wang, Q.; Bai, Z.; Li, Y.; Jia, R.; Li, X. Simulation on Petroleum Hydrocarbon Pollutants Transport Law and Hydrodynamic Interception Technology of an Oil Depot. *Saf. Environ. Eng.* **2023**, *30*, 216.
25. Hong, C. Sorption of Petroleum Hydrocarbons on Soil and Sorption of Selected Organic Pollutants on Petroleum-Contaminated Soil. Ph.D. Thesis, Dalian University of Technology, Dalian, China, 2009.
26. Wang, X.P.; Lanning, L.M.; Ford, R.M. Enhanced Retention of Chemotactic Bacteria in a Pore Network with Residual NAPL Contamination. *Environ. Sci. Technol.* **2016**, *50*, 165–172. [CrossRef] [PubMed]

Disclaimer/Publisher's Note: The statements, opinions and data contained in all publications are solely those of the individual author(s) and contributor(s) and not of MDPI and/or the editor(s). MDPI and/or the editor(s) disclaim responsibility for any injury to people or property resulting from any ideas, methods, instructions or products referred to in the content.